# Reaction of nitrogen oxide (N2O5) with water on carbonaceous surfaces

**ARTICLE** *in* THE JOURNAL OF PHYSICAL CHEMISTRY · SEPTEMBER 1986

Impact Factor: 2.78 · DOI: 10.1021/j100410a025



**3 AUTHORS**, INCLUDING:

Ludwig Brouwer
Technische Universität Clausthal
**24** PUBLICATIONS **297** CITATIONS
SEE PROFILE

Michel J Rossi
Paul Scherrer Institut
**261** PUBLICATIONS **6,396** CITATIONS
SEE PROFILE

reactions on the surface of metal colloids all the adsorption sites were shown[38] to be catalytically active. This is probably not true of SERS active sites on colloidal metal particles. Single and primary metal particles have the same edges, corners, etc. that occur in clusters of particles, but do not exhibit any detectable SERS enhancements.

We have examined a model in which a chain aggregate was constructed by sharing faces, edges, or corners of decahedra. Between each pair of adjacent particles in the chain there are wedge-shaped cavities of variable apical angle in which faces, edges, and/or corners form parts of the wedge cavity. This particular set of shared faces, edges, and corners may represent the SERS active surface and also form a fractal curve. This is not inconceivable since the boundary of the face in a multifaceted crystal does form a fractal structure. The edges and corners do not represent discontinuities; rather they are smoothed over on the atomic scale by silver atoms of finite surface area. Much of the heterogeneity in adsorption of $CrO_4^{2-}$, $MoO_4^{2-}$, and $WO_4^{2-}$ on aggregates of silver particles, as reflected in the large bandwidths of SERS bands, probably arises from adsorption on different types of SERS active sites, i.e., faces, edges, and corners. For example, tridentate coordination of the oxoanion may be the preferred mode on a face, bidentate, on an edge, and monodentate, on a corner.

*Acknowledgment.* This work was supported by Army Research Office Grant DAAG29-85-K-0102, by NIH Grant GM-30904, and by NSF Grant CHE-801144. We thank Dr. Lee Guterman, who carried out the light-scattering measurements.

**Registry No.** PVP, 9003-39-8; AG 501-X8, 75444-61-0; $CrO_4^{2-}$, 13907-45-4; $MoO_4^{2-}$, 14259-85-9; $WO_4^{2-}$, 14311-52-5; Ag, 7440-22-4; sodium citrate, 994-36-5.

*Supplementary Material Available:* Figures 1′–4′ (4 pages) showing first-order rate dependence of surface Raman band intensity ($\Delta I$) and absorbance ($\Delta A$) on time in intermediate time range. Ordering information is given on any current masthead page.

(38) Turkevich, J. In *Heterogeneous Catalysis: Selected American Histories*; Davis, B. H., Hettinger, W. P., Jr., Eds.; ACS Symposium Series 22; Amercian Chemical Society: Washington, DC, 1983.

(39) In this paper the periodic group notation in parentheses is in accord with recent actions by IUPAC and ACS nomenclature committees. A and B notation is eliminated because of wide confusion. Groups IA and IIA become groups 1 and 2. The d-transition elements comprise groups 3 through 12, and the p-block elements comprise groups 13 through 18. (Note that the former Roman number designation is preserved in the last digit of the new numbering: e.g., III → 3 and 13.)

# Reaction of $N_2O_5$ with $H_2O$ on Carbonaceous Surfaces

**L. Brouwer,† M. J. Rossi,* and D. M. Golden**

*Department of Chemical Kinetics, Chemical Physics Laboratory, SRI International, Menlo Park, California 94025* *(Received: December 6, 1985; In Final Form: March 24, 1986)*

The heterogeneous reaction of $N_2O_5$ with commercially available ground charcoal in the absence of $H_2O$ revealed a physisorption process ($\gamma = 3 \times 10^{-3}$) together with a redox reaction generating mostly NO. Slow $HNO_3$ formation was the result of the interaction of $N_2O_5$ with $H_2O$ that was still adsorbed after prolonged pumping at $10^{-4}$ Torr. In the presence of $H_2O$, the same processes with $\gamma = 5 \times 10^{-3}$ are observed. The redox reaction dominates in the early stages of the reaction, whereas the hydrolysis gains importance later at the expense of the redox reaction. The rate law for $HNO_3$ generation was found to be $d[HNO_3]/dt = k_{bi}[H_2O][N_2O_5]$ with $k_{bi}$, the effective bimolecular rate constants, for 10 mg of carbon being $(1.6 \pm 0.3) \times 10^{-13}$ cm$^3$/s.

## Introduction

The chemistry of the atmosphere is generally thought of in terms of gas-phase reactions and photoprocesses, but given the presence of various particles and liquid droplets, the importance of certain competing heterogeneous processes has also been postulated.[1]

In the stratosphere, the collision frequency of a gas molecule with an average particle is about $10^{-5}$ s$^{-1}$, and thus very few processes, even if unit efficient, can compete with the gas-phase chemistry. However, it has been suggested[2] that some heterogeneous reactions of $N_2O_5$ might account for observed inconsistencies in the measured seasonal $NO_x$ variations.

In the troposphere, there are considerably more collisions between gas molecules and particles. The collision frequency in a highly polluted urban environment is about 1 s$^{-1}$, and loss processes with efficiencies of even $10^{-4}$ can compete with gas-phase processes.

Dinitrogen pentoxide, $N_2O_5$, is mainly formed through recombination of $NO_2$ and $NO_3$ radicals throughout the atmosphere, that is, from the lower troposphere to the stratosphere. However, the homogeneous reaction of $N_2O_5$ with $H_2O$ is slow due to the closed-shell nature of both reaction partners. An interesting possibility for the potential importance of the $N_2O_5$ hydrolysis to nitric acid in the atmosphere would be its catalysis on small aerosol particles with surfaces like carbonaceous material or sulfuric acid. A sufficiently rapid effective bimolecular rate constant for reaction 1 could make this process an important sink for $NO_x$.

$$N_2O_5 + H_2O \rightarrow 2HNO_3 \qquad (1)$$

In this work we investigate the interaction of gaseous $N_2O_5$ with a carbonaceous surface, in both the absence and presence of $H_2O$. Two questions were of prime interest to us: First, what is the nature of the products that result from this interaction? Second, if $HNO_3$ is a major product, what is its effective rate of formation due to a heterogeneous mechanism? Due to the fact that in this phase of our research we were primarily interested in the chemical aspect of this gas–surface interaction, we did not attempt detailed surface characterization. A simple commercially available carbon substrate was used. It was inevitable that the surface condition of the carbon sample changed over time, and therefore small changes in the quantitative parameters of the gas–solid interaction had to be expected. However, in no instance did this uncertainty affect the conclusions, and in general the self-consistency of the data is surprisingly good.

† Postdoctoral Research Associate. Present address: Institut für Physikalische Chemie, Universität Göttingen, West Germany.

(1) Heikes, B. G.; Thompson, A. M. *J. Geophy. Res. A* **1983**, *88*, 883.
(2) Ridley, B. A.; et al. *J. Geophys. Res., A* **1984**, *89*, 4797.

0022-3654/86/2090-4599$01.50/0 

We chose an experimental technique that was pioneered in our laboratories and essentially is a variation of the VLPP (very low pressure pyrolysis) method. We have explored a variety of heterogeneous reactions using this technique.[3,4] In this work, we extend this technique to the measurement of the catalysis of the effective bimolecular reaction between the title compounds. The next section describes our experimental technique in more detail, after which presentation and discussion of our results will ensue.

## Experimental Section

The experimental technique is a variation of the VLPP method, where a part of the vessel walls constitutes the active surface of interest. The VLPP technique has been described in detail elsewhere.[3-5] In short, a controlled flow of reactant gas enters a Knudsen cell reactor which contains two chambers connected by a large, sealable aperture. The lower chamber contains the reactive surface, and the upper chamber contains the reactant inlets and the escape aperture. The reactant and product gases are formed into an effusive molecular beam at the escape aperture, whose diameter can be chosen between two values without breaking the vacuum by means of a plunger-sliding seal arrangement. The molecular beam is modulated mechanically by using a tuning fork chopper and is monitored by a mass spectrometer (Balzers QMG 311) located in the second, differentially pumped vacuum chamber. The modulated portion of the ion current is recorded with a lock-in amplifier, whose dc output constitutes the primary observable in our experiment. Our method thus allows us to monitor the constituents of the molecular beam without interference from gas–wall collisions that occur after the molecules have left the Knudsen cell reactor.

When the aperture connecting the upper and lower chamber is opened, the extent of adsorption or reaction on the active surface may be easily measured from the change in mass spectral signal of the reactant or from the appearance of mass spectral signals of product molecules. This measurement can then simply be converted to an absolute rate constant.[4] This study was performed by using only one aperture (3-mm diameter) of the Knudsen cell, whose parameters are as follows: $k_e = 0.586 \times (T/M)^{1/2}\ s^{-1}$, $\omega = 639.3 \times (T/M)^{1/2}\ s^{-1}$, and $Z_w = 1.09 \times 10^3$, where $k_e$ is the escape rate constant for a species of mass $M$ at temperature $T$, $\omega$ the gas–wall collision frequency of the average molecule with the active surface in the second chamber, and $Z_w$ the corresponding collision number. The active surface area was a Pyrex plate of 66.5 $cm^2$ on which 10–11 mg of a representative prototype carbonaceous material was laid out. Except for the active surface in the second chamber, the reaction vessel was coated with halocarbon wax 15-00, in order to minimize heterogeneous reactions on the vessel walls other than the active surface. Following Baldwin,[2] we took a commercial ground charcoal (Norit A, North American Norit Co.), which had a measured BET surface area of 37 $m^2/g$. Therefore, our sample had a BET surface area of 3700 $cm^2$. All experiments were performed with this mass of ground charcoal in order to keep this parameter a constant. The samples were pumped for at least 4 h at $10^{-4}$ Torr prior to an experiment, and acceleration of the pumping process could be effected by heating the carbon. All experiments were done at room temperature using reagent grade gases where available.

Batches of dinitrogen pentoxide were prepared by the ozone oxidation of $NO_2$ in the gas phase in an excess of $O_3$. The synthesis was straightforward except for the fact that $H_2O$ had to be rigorously excluded from both reagents used in order to prevent any hydrolysis of $N_2O_5$ resulting in its contamination with $HNO_3$. As will be explained in the results section, the monitoring of $N_2O_5$ is only possible when dinitrogen pentoxide is free of $HNO_3$ or contaminated to the extent of only a few percent, because of grossly differing mass spectroscopic sensitivities at $m/e$ 62 ($NO_3^+$ for $N_2O_5$) and $m/e$ 63 ($HNO_3^+$ for $HNO_3$). This was achieved by passing both $O_3$ and $NO_2$ through $P_2O_5$ in order to remove $H_2O$. This treatment reduced the $HNO_3$ level in $N_2O_5$ to under 2%. The reaction vessel was passivated with gaseous $N_2O_5$ prior to collection at −78 °C, and the inlet system was kept as close as possible to the VLPP Knudsen cell. A gaseous batch of $N_2O_5$ could be kept for about 30 min before decomposition became important (pressure increase in inlet line). Typically, the dry ice trap was removed from the storage bulb that contained the white crystalline solid $N_2O_5$ until the pressure attained about 30 Torr in the inlet line, after which the storge container was isolated from the remainder of the inlet line and stored at dry ice temperature. Under those conditions the solid dinitrogen pentoxide could be used for several days with $HNO_3$ impurity levels of less than 2%.

**TABLE I: Balzers QMG-311 Mass Spectrometric Fragmentation Pattern upon Electron Impact (70 eV) for $HNO_3$ and $N_2O_5$ (with <3% $HNO_3$ Impurity)[a]**

| | mass spectra | | | | | |
|---|---|---|---|---|---|---|
| | 14 | 16 | 30 | 46 | 62 | 63 |
| $HNO_3$ | 8.8 | 17.7 | 83 | 100 | | 1.1 |
| $N_2O_5$ | 5.8 | 13.5 | 73.6 | 100 | 0.013 | |

[a] The sensitivity ratio of $HNO_3$ to $N_2O_5$ is 0.38 ± 0.10 at $m/e$ 46. Unit mass resolution, $m/e$ 63.

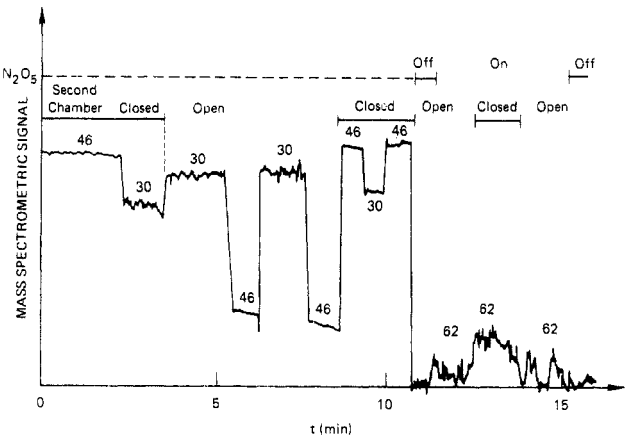


**Figure 1.** The system $N_2O_5$ on carbon without flowing $H_2O$. Mass spectral information as a function of time and experimental configuration of the Knudsen cell reactor.

## Results and Discussion

*$N_2O_5$ on Carbon in the Absence of $H_2O$.* The mass spectrum of $N_2O_5$ does not have a parent peak ($m/e$ 108) under our experimental conditions. Its highest mass fragment peak can be found at $m/e$ 62 corresponding to $NO_3^+$, and Table I presents the mass spectral fragmentation pattern for our mass spectrometer conditions. From the relative intensity it can be seen that selective monitoring of $N_2O_5$ at $m/e$ 62 is only possible at high flow rates of dinitrogen pentoxide into the reactor. In order to study the adsorption behavior of $N_2O_5$ on carbon, we flowed it into the cell at a rate of $(1.3–4) \times 10^{17}$ molecules/s and observed the different mass spectrometric signals displayed in Figure 1. With $1.3 \times 10^{17}$ molecules of $N_2O_5$/s flowing into the reactor and the second chamber open, that is, the carbon exposed to the reactive gas flow, the signal at $m/e$ 62 decreases to about 30% of its original value. When one watches its long-term behavior, it increases to its original value (second chamber closed) in a matter of a few minutes. The signal at $m/e$ 46 behaves in a very similar manner, whereas the signal at $m/e$ 30 shows the opposite effect. In another experiment with a fresh carbon sample, the $m/e$ 62 signal decreased to 25% of its original value at a flow rate of $4 \times 10^{17}\ s^{-1}$. This corresponds to a sticking coefficient of $3 \times 10^{-3}$ if the geometric surface area over which the carbon sample was laid out is taken into account. However, the signal level approaches 90% of its original level after 5 min, which indicates saturation of the carbon sample by $N_2O_5$. An approximate calculation indicates that about 10 monolayers of $N_2O_5$ molecules are adsorbed at saturation using the above high

(3) Baldwin, A. C. *Int. J. Chem. Kinet.* **1982**, *14*, 269 and references therein.
(4) Baldwin, A. C.; Golden, D. M. *Science* **1979**, *206*, 562.
(5) Golden, D. M.; Spokes, G. N.; Benson, S. W. *Angew. Chem.* **1973**, *12*, 354.

flow rates. When $HNO_3$, which is always present as a minor impurity, was monitored at $m/e$ 63 in the same experiment, an initial decrease of 10–15% was followed by an increase until it reached a level larger by a factor of 2 with respect to the original level with the second chamber closed. Apparently, $HNO_3$ was being generated in a slow process after the initial adsorption of the $HNO_3$ impurity in $N_2O_5$, by using $H_2O$ that remained adsorbed even on the "fresh" carbon sample. This water reservoir can be released into the gas phase when the carbon sample is heated for a certain period of time during which $H_2O$ and CO are released into the gas phase. No $CO_2$ or hydrocarbons (up to mass 300) have been detected. Furthermore, when an $N_2O_5$-saturated carbon sample is heated, the signal at $m/e$ 62 increases when the dinitrogen pentoxide source has been turned off. Thus, some of the $N_2O_5$ is physisorbed and retains its molecular integrity on the carbon for some time before it reacts with carbon or with adsorbed water. It seems, thus, that the mentioned surface reactions of $N_2O_5$ are slow on the time scale of our experiment. The observed signal could conceivably come also from the $NO_3$ radical which could be a decomposition product of $N_2O_5$ on the carbon surface. However, we find this possibility to be remote because of the well-known tendencies of many polyatomic radicals to undergo surface reactions.

The interpretation of the data shown in Figure 1 can be summarized as follows: First, instantaneous adsorption of $N_2O_5$ takes place to about 75%. A slow hydrolysis reaction resulting in $HNO_3$ with adsorbed $H_2O$ ensues. Second, the mass spectrum indicates not only an adsorptive loss of $N_2O_5$ but also a reaction on the carbon as evidenced by the strong decrease in the ratio of the mass spectral peaks at $m/e$ 46–30. This increase in the intensity of the $m/e$ 30 peak strongly suggests the formation of NO as decomposition product of the nitric acid anhydride and therefore suggests a redox reaction that takes place on the same time scale as the adsorption of $N_2O_5$. The nature of this product indicates that the carbon is being oxidized upon its exposure to the nitric acid anhydride. This situation is very similar to the $NO_2$ interaction with the same carbon substrate, where NO is generated in the absence of $H_2O$ in addition to the purely adsorptive loss of $NO_2$.[6] Furthermore, from Figure 1 and additional data, we deduce that $NO_2$ is not a major reaction product, and we can give an upper limit of 10% with respect to the abundance of NO.

*$N_2O_5$ on Carbon in the Presence of $H_2O$.* At high flow rates of both $H_2O$ and $N_2O_5$ large quantities of $HNO_3$ are detected by using $m/e$ 63. It turns out that the detection of both $N_2O_5$ and $HNO_3$ in the same system is possible in view of the minimal interference of $m/e$ 62 corresponding mainly to $N_2O_5$ with $m/e$ 63 ($HNO_3$). Earlier calibration experiments in our laboratory established a ratio of >500 for $m/e$ 62–63 for $HNO_3$. Table I displays those facts in a quantitative manner.

Five mass spectrometric signals, $m/e$ 63, 62, 46, 30, and 18, were recorded as a function of $N_2O_5$ exposure time with $H_2O$ flowing into the reactor. As indicated above, $m/e$ 63 is representative of $HNO_3$, while $m/e$ 62 and 46 are representative of $N_2O_5$. In high flow rate experiments ($F^i(N_2O_5) \sim 10^{17}$ molecules/s) where all of the above signals could be monitored simultaneously, $NO_2$ formation was absent to the extent of an upper limit of 10% of $HNO_3$. Changes in $m/e$ 46 corresponded quantitatively to changes in 62 when the $HNO_3$ contribution to $m/e$ 46 was taken into account. For the quantative experiments at lower flow rates of $N_2O_5$, it was thus assumed that no $NO_2$ resulted from the $N_2O_5/H_2O/C$ interaction, so that the more intense $m/e$ 46 could be used as a monitor for the $N_2O_5$ concentration. The absence of any major amounts of $NO_2$ also follows from the quantitative agreement in the mass balance (vide infra) which shows the stoichiometric relationship between $N_2O_5$ loss (measured at $m/e$ 46) and $H_2O$ loss with respect to the $HNO_3$ production. The signal at $m/e$ 30 was corrected for the $HNO_3$ and $N_2O_5$ contribution and indicated the extent of NO formation, while $m/e$ 18 was representative of the steady-state $H_2O$ levels in the reaction vessel.

(6) Brouwer, L., unpublished results.

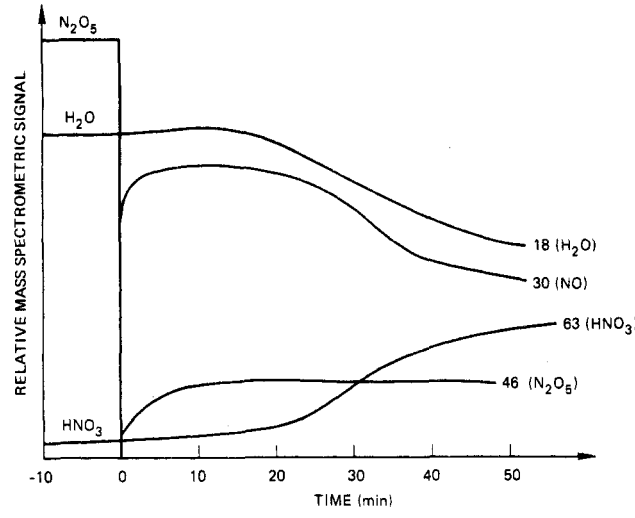


**Figure 2.** Time evolution of $H_2O$ (18), $N_2O_5$ (46), $HNO_3$ (63), and NO (30) in the system $N_2O_5/H_2O$ on carbon, assuming no $NO_2$ is formed. Signal level for $m/e$ 46 starts at the upper horizontal line. $F^i(N_2O_5) = 1.7 \times 10^{16}$ and $F^i(H_2O) = (1-2) \times 10^{16}$ molecules/s.

In order to measure the hydrolysis product, $HNO_3$, quantitatively, it became necessary to conduct reference experiments of the interaction of $HNO_3$ with the same carbon substrate. Dry $HNO_3$ was flowed into the VLPP reactor, and its concentration was monitored by using $m/e$ 63. The behavior of $HNO_3$ on carbon in the absence of $H_2O$ can be summarized as follows: $HNO_3$ undergoes both adsorption as well as reduction to NO and $NO_2$ in an apparent redox reaction, whereby the carbon acts as the reducing agent. However, the NO and $NO_2$ evolution stops within 5–30 min (depending on the flow rate) before saturation of the carbon substrate with $HNO_3$ is complete. This apparently has to do with exhaustion of the available redox sites before all the adsorption sites are occupied. This point is also borne out in repetitive $HNO_3$ exposure experiments, where the carbon has had a chance to recover between experiments. Here the total number of adsorbed $HNO_3$ molecules and the redox products decrease with each repetitive experiment. In other words, both reaction channels—total disappearance due to adsorption and reduction to NO and $NO_2$—track each other. Furthermore, fresh carbon samples show a complex time dependence of NO and $NO_2$ production with a maximum in the rate of formation showing up a short while after the start of the reaction.

The time dependence of the mass spectrum resulting from the interaction of $N_2O_5$ with carbon in the presence of $H_2O$ is displayed in Figure 2. The flow rates of both reactants were high (approximately $2 \times 10^{16}$ molecules/s) in order to be able to follow the concentrations of all the important species. However, the flow rate was not high enough to monitor the $N_2O_5$ concentration through its fragment peak at $m/e$ 62. Figure 2 shows the presence of NO along with the changing concentrations of $H_2O$, $HNO_3$, and $N_2O_5$, indicating that even under these "wet" conditions some oxidation/reduction chemistry is taking place on the carbon surface. It appears that the first few minutes in the product appearance spectrum resemble closely the $N_2O_5/C$ interaction in the absence of water (vide supra).

The signals have been corrected for the small $HNO_3$ impurity in $N_2O_5$ as well as the amount of $HNO_3$ generated on the vessel walls that have been coated with halocarbon wax which should prevent or at least minimize the wall deactivation of $N_2O_5$ on surfaces other than the surface of interest. All the mass spectrometric signals displayed in Figure 2 have been corrected appropriately with the aid of authentic mass spectra. Furthermore, the critical reference experiment has been performed where the lower chamber that usually holds the carbon sample was exposed to the same $N_2O_5/H_2O$ mixture in the absence of carbon. No increase in the $HNO_3$ and NO partial pressure was detected so that we conclude that the presence of carbon is necessary in order to generate the products shown in Figure 2. As a result, the carbon

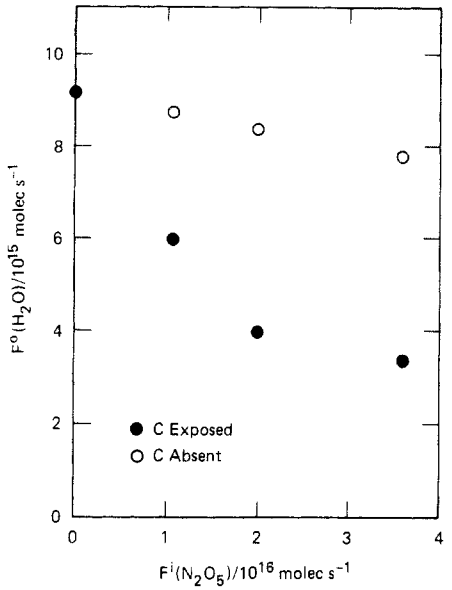


**Figure 3.** $H_2O$ flow rates out of the Knudsen cell as a function of $N_2O_5$ flow rate at constant $H_2O$ flow rate of $9.2 \times 10^{15}$ molecules/s: ●, C exposed; ○, C absent.

surface is a specific catalyst for the observed reaction products.

At the given flow rates for $N_2O_5$ and $H_2O$ the carbon sample reaches a steady state after approximately 10 min, which corresponds to about one monolayer coverage in the presence of $H_2O$. Once that $N_2O_5$ coverage and steady-state condition has been achieved, 17% of the $N_2O_5$ passes the reactor unchanged or 83% is lost irreversibly on the carbon surface corresponding to $\gamma = 5 \times 10^{-3}$. Obviously, the two chemical reactions— adsorption and the redox reaction—are occurring simultaneously, a fact that is also apparent when one considers the signal at $m/e$ 30. The NO production starts right after the second chamber has been opened, whereas the $H_2O$ consumption and the appearance of the hydrolysis product $HNO_3$ follow at a later stage. It seems that the hydrolysis becomes important at the expense of redox reaction because the NO signal tracks the consumption of the $H_2O$ signal very well. The appearance of $HNO_3$ seems to be delayed even further because nitric acid has to saturate specific sites on the carbon before significant desorption, and therefore observation by mass spectrometry can take place.

The conclusion of this qualitative part of our study can be stated as follows: First, adsorbed $N_2O_5$ can either oxidize the carbon and form NO or react with $H_2O$ to yield $HNO_3$. Second, after the adsorption of $N_2O_5$ is saturated, a constant fraction (83%) is consumed in the reactor by oxidation, hydrolysis, or physisorption. Third, initially, the oxidation of carbon is the main reaction. At later stages the hydrolysis increases in importance and eventually becomes dominant.

Additional information can be obtained when the $H_2O$ partial pressure is monitored at $m/e$ 18 with both $H_2O$ and $N_2O_5$ flowing into the reactor. When the carbon sample is saturated with $H_2O$ vapor, corresponding to approximately one monolayer, and subsequently exposed to a high flow rate of both reactants, the $H_2O$ partial pressure drops significantly to a new steady-state level, which is a function of both the $H_2O$ and the $N_2O_5$ flow rate. Figure 3 displays a data set where the carbon has been saturated with a flow of $9 \times 10^{16}$ molecules/s of $H_2O$. Furthermore, the saturation behavior of $H_2O$ shows a complex time dependence in the presence of $N_2O_5$ and carbon in that the water partial pressure shows a maximum between the start of the surface reaction and steady state. It is as if the $N_2O_5$ displaces additional $H_2O$ that saturated the surface of the carbon sample. This maximum in the $H_2O$ partial pressure is similar to the one found in the $HNO_3$/C interaction in the absence of $H_2O$ (vida supra).

Noteworthy is the fact that even in the absence of the carbon some hydrolysis is taking place, presumably on the walls of the reaction vessel, and its importance apparently increases with increasing flow rate of $N_2O_5$. However, the above reference

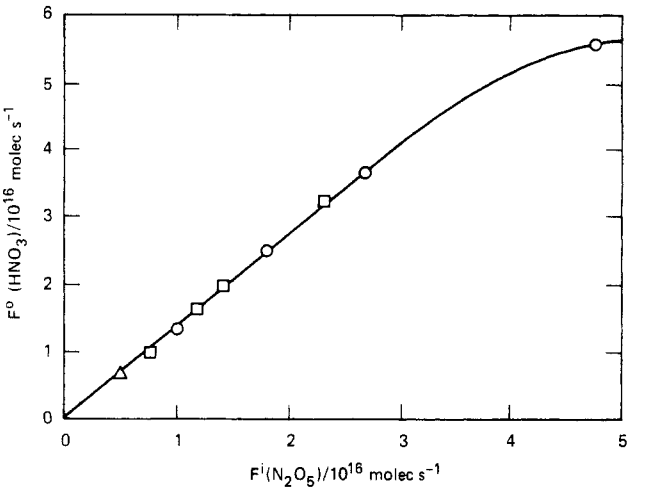


**Figure 4.** $N_2O_5/H_2O$ on carbon: variation of product flux ($HNO_3$) as a function of $N_2O_5$ flow rate under $H_2O$-rich conditions. $F^i(H_2O)$: ○, $1.2 \times 10^{17}$; □, $6.0 \times 10^{16}$; △, $2 \times 10^{16}$ molecules/s.

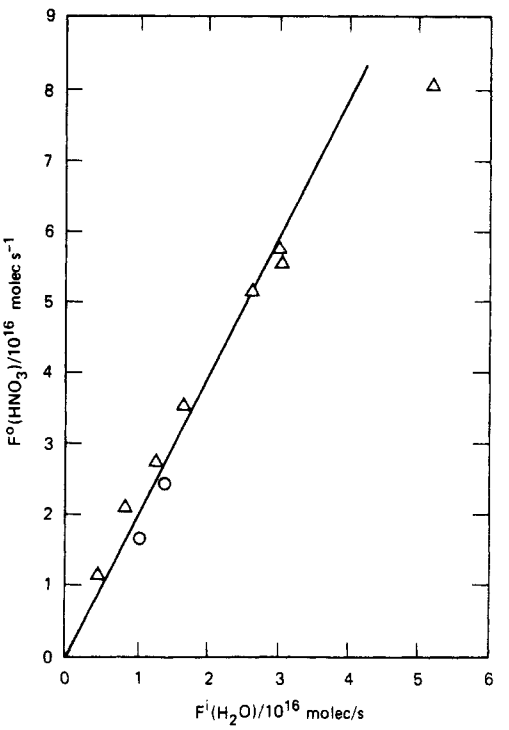


**Figure 5.** $HNO_3$ generation in the system $N_2O_5/H_2O$ on carbon under $N_2O_5$-rich conditions. $F^i(N_2O_5)$: △, $5 \times 10^{16}$; ○, $1.25 \times 10^{16}$ molecules/s.

experiment shows clearly that the surface of the reaction chamber, excluding the active carbon surface, does not lead to increased surface reaction of $N_2O_5$.

This reaction system offers the unique opportunity to study all reaction channels in detail. The $H_2O$ depletion monitored at $m/e$ 18 monitors the hydrolysis rate ($k_{bi}$) of $N_2O_5$ exposed to carbon. The detection of the $HNO_3$ signal affords the opportunity to cross-check the hydrolysis reaction, whereas the NO detection yields information upon the concurrent oxidation of carbon by $N_2O_5$ in the presence of $H_2O$. Finally, the $N_2O_5$ depletion monitored at $m/e$ 62 or 46 (for lower flow rates) measures the total disappearance due to physisorption, redox reaction, and hydrolysis of $N_2O_5$ and can be described by the sticking coefficient $\gamma$.

The appearance of the hydrolysis product $HNO_3$ has been found to be linearly dependent on both $N_2O_5$ (Figure 4) and $H_2O$ (Figure 5). The goal of these studies was to find the rate law for formation of $HNO_3$, and both plots show a simple linear relationship as long as the constant component was in sufficient excess with respect

**TABLE II: Mass Balance Data**[a]

| $F^i(H_2O)$ | $F^\circ_c(H_2O)$ | $F^\circ(H_2O)$ | $F^r(H_2O)$ | $F^\circ(HNO_3)$ | $F^\circ_c(HNO_3)$ | $F^n(HNO_3)$ | $F^i(N_2O_5)$ | $F^\circ(N_2O_5)$ | $F^r(N_2O_5)$ |
|---|---|---|---|---|---|---|---|---|---|
| 2.8 | 2.5 | 0.5 | 2.0 | 9.0 | 4.0 | 5.0 | 28.0 | 18.0 | 10.0 |
| 5.8 | 5.5 | 1.5 | 4.0 | 13.0 | 4.5 | 8.5 | 28.0 | 16.5 | 11.5 |
| 8.5 | 8.0 | 2.5 | 5.5 | 17.0 | 5.0 | 12.0 | 28.0 | 14.5 | 13.5 |
| 9.8 | 8.5 | 2.5 | 6.0 | 16.5 | 3.5 | 13.0 | 28.0 | 14.0 | 14.0 |

[a] Mass balance data for $N_2O_5 + H_2O$ on 11 mg of carbon under $N_2O_5$-rich conditions, as a function of $H_2O$ flow rate. All flows are in $10^{15}$ $s^{-1}$; $F^i$ is flow into the reactor, $F^\circ_c$ is flow out with second chamber closed, $F^\circ$ is the flow out of reactor, $F^r$ is flow of reacted molecules, and $F^n(HNO_3)$ is net flow of $HNO_3$ out, corrected for $HNO_3$ formed in the absence of the active carbon surface. $H_2O$ was monitored at 18 amu, $HNO_3$ at 63 amu, and $N_2O_5$ at 46 amu.

to the varied component in order to maintain pseudo-first-order conditions. The variation of the $HNO_3$ concentration as a function of $F^i(N_2O_5)$ under $H_2O$-rich conditions (Figure 4) reveals that approximately $^2/_3$ of the $N_2O_5$ flowing in ends up as $HNO_3$ that desorbs and is therefore monitored. However, about $^2/_3$ of the $N_2O_5$ flowing into the reactor is also consumed on the surface under those conditions so that nearly all of the adsorbed $N_2O_5$ is converted into $HNO_3$ under steady-state conditions. The quantitative aspects will be discussed in terms of the mass balance (vide infra). The emphasis of the data displayed in Figures 4 and 5 is to derive the rate law given below. The variation of the $HNO_3$ concentration as a function of $F^i(H_2O)$ under $N_2O_5$-rich conditions (Figure 5) shows that stoichiometric amounts of $HNO_3$ are formed with respect to the depletion of $H_2O$: For every 2 mol of $HNO_3$ formed 1 mol of $H_2O$ is consumed. This is a consequence of the fact that the carbon was already saturated with $H_2O$ prior to the experiment and the water flow into the VLPP reactor serves only to replace that amount of $H_2O$ that is consumed in the course of the $N_2O_5$ hydrolysis. The results shown in Figures 4 and 5 determine the rate law given in eq 2 for the hydrolysis reaction given

$$d[HNO_3]/dt = k_{bi}[H_2O][N_2O_5] \quad (2)$$

in eq 1. It must be made clear, however, that this is an effective biomolecular rate constant which almost certainly is dependent upon the mass of the carbon. We did not intend to study the mass dependence of this rate constant, so it must be kept in mind that the numerical value refers to a mass of about 10 mg of carbon of the specified brand. The numerical value for $k_{bi}$ can be calculated according to the equation

$$k_{bi} = 0.5F^\circ(HNO_3)/[H_2O][N_2O_5] \quad (3)$$

where $F^\circ(HNO_3)$ is the flow of $HNO_3$ out of the Knudsen cell and where the terms in brackets are the gas-phase concentrations of the corresponding species. Using our experimental data, we find $k_{bi} = (1.6 \pm .3) \times 10^{-13}$ $cm^3/s$, which is very fast indeed. Equation 3 has been derived from a reaction mechanism that brings together the two adsorbed species $HNO_3$ and $N_2O_5$ on the carbon surface. The kinetics has been derived for saturation coverages of both reactants because it conformed to the actual experimental situation. In case the rate constant has to be estimated for low coverages, the given number can be regarded as a lower limit.

The last experiment concerns the mass balance, which is a critical test for the validity of a proposed reaction scheme. Table II presents mass balane data which are plotted in Figure 6. It can be seen that there is a 1:1 correspondence between $H_2O$ and $N_2O_5$ consumed under the present "wet" conditions. By extrapolation, one can see that without $H_2O$ flowing into the reactor but maintaining $H_2O$-saturated conditions on the carbon, $8 \times 10^{15}$ molecules/s of $N_2O_5$ are consumed out of the $2.8 \times 10^{16}$ molecules/s flowing into the reactor. These molecules constitute that portion of $N_2O_5$ (29%) which undergoes reduction to NO by the carbon and physisorption. Moreover, there is little $HNO_3$ formed under the same conditons of no net $H_2O$ flow into the reactor, and it amounts to approximately $1.5 \times 10^{15}$ molecules/s. The $HNO_3$ production rate picks up linearly with increasing $H_2O$ flow into the reactor as does the $H_2O$ consumption rate. The "excess"

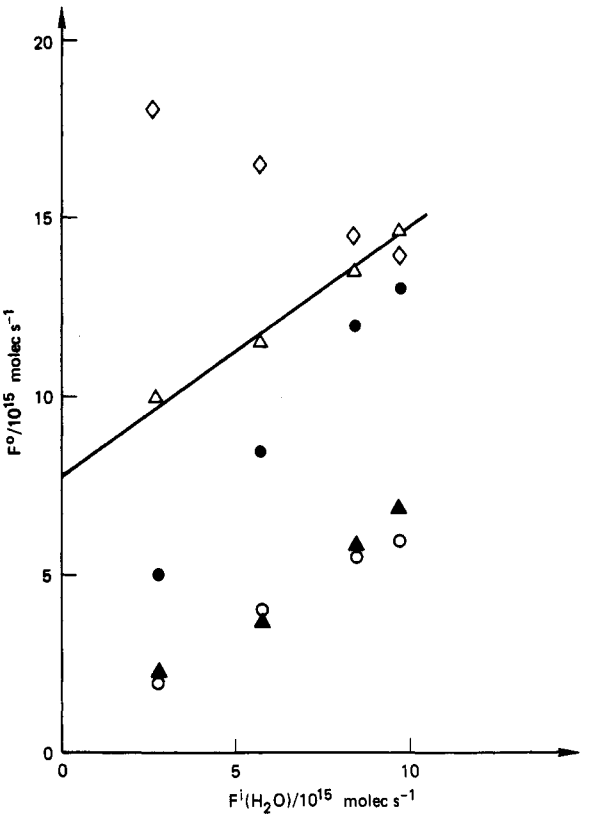


**Figure 6.** Mass balance in the system $N_2O_5/H_2O$ on carbon under $N_2O_5$-rich conditions as a function of $H_2O$ flow rate into the Knudsen cell: ○, consumed $H_2O$; ●, formed $HNO_3$; △, consumed $N_2O_5$; ◇, $N_2O_5$ remaining; ▲, "excess" consumed $N_2O_5$. $F^i(N_2O_5) = 2.8 \times 10^{16}$ molecules/s.

consumed $N_2O_5$ is that portion which is converted into $HNO_3$ above the amount that is physisorbed and/or reduced by the carbon. The excellent mass balance and the stoichiometric relationship between "excess" consumed $N_2O_5$, consumed $H_2O$, and formed $HNO_3$ together with the simplicity of the rate law for heterogeneous hydrolysis give us good confidence in our results.

*Atmospheric Significance.* At this stage, the atmospheric significance must be limited to a statement that the reaction between $N_2O_5$ and $H_2O$ to form $HNO_3$ is catalyzed by carbonaceous material. If the charcoal material used here is at all similar to atmospheric carbonaceous matter, there are strong grounds for considering such processes in atmospheric models. In the future, we hope to investigate the effect of changing the carbonaceous matter and the temperature. We will also employ some surface characterization techniques to examine the difference between carbon samples.

*Acknowledgment.* This work was supported in part by Contract DE-AC03-78-EV10121 of the U.S. Department of Energy and Contract NASW-3888 of the National Aeronautics and Space Administration.

**Registry No.** $N_2O_5$, 10102-03-1; $H_2O$, 7732-18-5.